The Diabetes Gene and Wnt Pathway Effector TCF7L2 Regulates Adipocyte Development and Function

Xi Chen,[1] Iriscilla Ayala,[1] Chris Shannon,[1] Marcel Fourcaudot,[1] Nikhil K. Acharya,[2] Christopher P. Jenkinson,[3] Sami Heikkinen,[4] and Luke Norton[1]

Diabetes 2018;67:554–568 | https://doi.org/10.2337/db17-0318

The gene encoding for transcription factor 7-like 2 (*TCF7L2*) is the strongest type 2 diabetes mellitus (T2DM) candidate gene discovered to date. The TCF7L2 protein is a key transcriptional effector of the Wnt/β-catenin signaling pathway, which is an important developmental pathway that negatively regulates adipogenesis. However, the precise role that TCF7L2 plays in the development and function of adipocytes remains largely unknown. Using a combination of in vitro approaches, we first show that TCF7L2 protein is increased during adipogenesis in 3T3-L1 cells and primary adipocyte stem cells and that TCF7L2 expression is required for the regulation of Wnt signaling during adipogenesis. Inactivation of TCF7L2 protein by removing the high-mobility group (HMG)-box DNA binding domain in mature adipocytes in vivo leads to whole-body glucose intolerance and hepatic insulin resistance. This phenotype is associated with increased subcutaneous adipose tissue mass, adipocyte hypertrophy, and inflammation. Finally, we demonstrate that *TCF7L2* mRNA expression is downregulated in humans with impaired glucose tolerance and adipocyte insulin resistance, highlighting the translational potential of these findings. In summary, our data indicate that TCF7L2 has key roles in adipose tissue development and function that may reveal, at least in part, how TCF7L2 contributes to the pathophysiology of T2DM.

The human transcription factor 7-like 2 gene (*TCF7L2*) is the strongest candidate gene for type 2 diabetes mellitus (T2DM) (1). Intronic single nucleotide polymorphisms (SNPs) within *TCF7L2* consistently have been linked to an array of phenotypes related to T2DM (2,3). However, what effect TCF7L2 has on the development and function of adipose tissue remains to be fully elucidated.

In a landmark study by the MacDougald laboratory, expression of the Wnt pathway activator, Wnt1, in preadipocyte cell lines potently blocked adipogenesis (4). Follow-up experiments demonstrated that pharmacological activation of Wnt signaling stabilized β-catenin and blocked preadipocyte differentiation (4,5). Conversely, inhibition of Wnt signaling stimulates adipogenesis through a β-catenin–dependent pathway (6,7), and cross talk between β-catenin and key transcriptional regulators of adipogenesis has been demonstrated (7,8). Moreover, in multipotent precursors of the mesenchymal lineage, activation of Wnt/β-catenin stimulates osteoblastogenesis and inhibits adipogenesis (9). The consensus from these studies is that Wnt signaling inhibits adipogenesis and that β-catenin is a critical mediator of this effect.

Consistent with an inhibitory effect of Wnt activation on adipogenesis, overexpression of TCF7L2 lacking its β-catenin binding domain promotes adipogenesis in preadipocytes and in L6 myotubes (4,10). In humans, obesity interacts with the *TCF7L2* risk allele to enhance T2DM prevalence in nonobese subjects (11,12), and the *TCF7L2* gene is differentially methylated in adipose tissue of patients with T2DM (13). Moreover, weight loss after gastric bypass surgery led to differential expression of *TCF7L2* mRNA isoforms in subcutaneous fat biopsy samples. The expression of short *TCF7L2* isoforms was also more prevalent in patients with T2DM, suggesting an important role for *TCF7L2* alternative splicing in adipose tissue (14).

Despite these findings, key questions regarding the molecular and physiological role of TCF7L2 in adipose tissue

[1]Diabetes Division, University of Texas Health Science Center, San Antonio, TX
[2]Diabetes and Obesity Center of Excellence, University of Washington, Seattle, WA
[3]South Texas Diabetes and Obesity Institute, University of Texas Rio Grande Valley, Harlingen, TX
[4]Institute of Biomedicine, University of Eastern Finland, Kuopio, Finland
Corresponding author: Luke Norton, nortonl@uthscsa.edu.

Received 14 March 2017 and accepted 28 December 2017.

This article contains Supplementary Data online at http://diabetes.diabetesjournals.org/lookup/suppl/doi:10.2337/db17-0318/-/DC1.

remain. For example, it is not known whether TCF7L2 expression is regulated during adipogenesis, whether TCF7L2 protein levels are important to adipocyte development, or how TCF7L2 interacts with Wnt signaling in developing adipocytes. The physiological effect of TCF7L2 loss of function in adipocytes also remains to be elucidated, and at the genomic level, which genes TCF7L2 regulates in adipocytes is not known. These are important studies that may reveal novel functions of TCF7L2 that may help us understand the association between *TCF7L2* SNPs and T2DM risk.

In preliminary studies, we observed that TCF7L2 protein levels increased during adipogenesis in 3T3-L1 cells. Because this appeared inconsistent with the paradigm of TCF7L2-mediated inhibition of adipogenesis, we further explored the role of TCF7L2 in adipose tissue in vitro and in vivo. The data described in the current study suggest that TCF7L2 may, in fact, be required for adipogenesis and that its expression is important for the regulation of Wnt/β-catenin signaling during adipocyte development. Postdevelopment, blocking the transcriptional activity of TCF7L2 in rodent adipose tissue leads to subcutaneous adipocyte hypertrophy, whole-body glucose intolerance, and hepatic insulin resistance. Finally, we demonstrate that adipose tissue expression of *TCF7L2* is lower in human subjects with impaired glucose tolerance (IGT) and adipocyte insulin resistance. These findings highlight new and complex roles for TCF7L2 in adipose tissue development and function and further uncover novel mechanisms by which this important transcription factor may contribute to obesity and T2DM.

RESEARCH DESIGN AND METHODS

Cell Culture

Early passage 3T3-L1 cells were differentiated using standard procedures in the absence of thiazolidinediones (15). Primary adipocyte stem cells (ASCs) were isolated from inguinal fat pads of mice (4–6 weeks old) and differentiated into adipocytes, as described previously (16). Triglyceride accumulation was quantitated using a commercial assay (Abcam, Cambridge, U.K.). For the Wnt/β-catenin pathway inhibition experiments, IWR-1-endo was purchased from Selleck Chemicals (Houston, TX) and used at a final concentration of 10 μmol/L. Protein content was determined using the bicinchoninic acid assay, and cell number was analyzed using the TC10 automated cell counter (Bio-Rad, Hercules, CA).

TCF7L2 Lentiviral Short Hairpin RNA

Stable silencing of *Tcf7l2* mRNA was performed in low passage 3T3-L1 fibroblasts (passage 2) using SMARTvector (Dharmacon, Lafayette, CO) lentiviral short hairpin (sh)RNAs. Puromycin selection was used to isolate a heterogeneous cell population postinfection. Additional stable clones were generated using alternate plasmids and shRNA sequences that targeted different regions of the *Tcf7l2* gene. All shRNA sequences used in this study are provided in Supplementary Fig. 1.

Insulin-Stimulated Glucose Uptake

Glucose uptake in differentiated (day 8) adipocytes was quantitated using [^{3}H]2-deoxyglucose during a 30-min insulin incubation (200 nmol/L) (17). Data were corrected for negative control wells treated without insulin or cytochalasin B, or both.

Western Blot Analysis

Western blotting was performed as previously described (18). Membranes were probed with the following antibodies, all supplied by Cell Signaling Technology (Danvers, MA): TCF7L2 (number 2569), β-catenin (number 8480), nonphosphorylated Ser33/37/Thr41 (active) β-catenin (number 8814), total AKT (number 4691), phosphorylated (p)Ser473 AKT (pAKT) (number 4060), C/EBPβ (number 3087), C/EBPδ (number 2318), C/EBPα (number 2295), peroxisome proliferator–activated receptor-γ (PPAR-γ; number 2435), and fatty-acid-binding proteins (FABP) 4 (number 2120). The β-tubulin antibody (ab6046) was from Abcam (Cambridge, MA).

RNA Sequencing and Pathway Enrichment Analysis

RNA sequencing (RNA-Seq) was performed on shSCR and shTCF7L2 3T3-L1 cells at multiple times during adipogenesis and analyzed as previously described (18). Differentially expressed genes were required to have a false discovery rate (FDR) q value of <0.05 when comparing the shTCF7L2 against shSCR cells. Pathway enrichment analysis was performed using Gene Set Enrichment Analysis (GSEA). Raw sequencing data are available online (GEO accession number: GSE95029).

Animals

All animal procedures were approved by the Institutional Animal Care and Use Committee at University of Texas Health Science Center at San Antonio. Mice with LoxP sites flanking exon 11 of the mouse *Tcf7L2* gene have been described elsewhere (19). Adiponectin-Cre (Adipoq-Cre) mice were obtained from The Jackson Laboratory (stock # 010803) (Bar Harbor, ME). LoxP/LoxP littermate controls were used in all experiments. Mice were fed a standard chow or, starting at 8 weeks of age, a 60% high-fat diet (HFD; Research Diets, D12492).

Mouse Physiological Studies

Intraperitoneal (IP) glucose tolerance tests (IPGTT) and insulin tolerance tests (ITT) were performed essentially as previously described (20). For IPGTTs, mice were fasted for 10 h and 2 g/kg (3-month-old mice) or 50 mg (HFD-fed mice) was given IP. For ITT, mice were fasted for 5 h and a dose of 0.8 units/kg was given IP. Low-dose (1.5 mU $\cdot$ m^{-2} $\cdot$ min^{-1}) hyperinsulinemic-euglycemic clamps were used to assess hepatic insulin sensitivity in 3-month-old control and TCF7L2-mutant mice (ΔE11-TCF7L2). Clamp data were normalized to total body weight. Indirect calorimetry was performed using Promethion (Sable Systems, North Las Vegas, NV; 3-month-old mice) or TSE LabMaster (TSE Systems, Chesterfield, MO; 6-month-old mice) metabolic cages. Differences in energy expenditure were assessed using the National Institute of Diabetes and Digestive and Kidney Diseases Mouse Metabolic Phenotyping Centers ANCOVA method (21). Body composition was assessed using a Minispec

nuclear magnetic resonance analyzer (Bruker, Billerica, MA). Adipocyte size determination was performed on formalin-fixed adipose tissue using Adiposoft software (22).

Human Studies

All studies involving human subjects were approved by the University of Texas Health Science Center at San Antonio Institutional Review Board. Fasting abdominal subcutaneous adipose tissue specimens were obtained from subjects with and without adipose tissue insulin resistance (Adipo-IR), as previously described (23). All subjects underwent a standard 2-h oral GTT to confirm normal glucose tolerance (NGT) or impaired glucose tolerance (IGT). Fasting Adipo-IR was calculated from free fatty acid and insulin data (24). Adipose tissue RNA was extracted using standard protocols, and quantitative real-time PCR was performed for TCF7L2, as previously described (18).

Statistical Tests

Data are presented as univariate scatter plots or line graphs, with corresponding mean ± SD. GraphPad Prism 7.03 software was used for all statistical analyses. Data normality was assessed for in vivo experiments using the Shapiro-Wilk test, and nonparametric Mann-Whitney tests were used when deviations from normality were detected. Student two-tailed *t* tests were used for analysis between two groups of equal variances, and Welch *t* tests were used when the *F* test of equal variance failed. Data containing three or more groups were analyzed using one- or two-way ANOVA (adjusted for repeat measures where appropriate) with Holm-Šidák post hoc testing accounting for multiple comparisons, where appropriate.

RESULTS

TCF7L2 Expression During Adipogenesis

We first quantitated protein levels of TCF7L2 during adipogenesis in 3T3-L1 cells. The TCF7L2 antibody recognizes an epitope around Leu331 (exon 9) of human TCF7L2 and thus detects all protein isoforms of TCF7L2, although only 78 and 58 kDa proteins were detected. Although both protein isoforms increased significantly during adipogenesis and there was a strong correlation between them ($r = 0.95$, $P < 0.001$), the expression of the 58 kDa protein was significantly higher in fully differentiated adipocytes (Fig. 1*A–C*). We measured mouse *Tcf7l2* mRNA using a TaqMan probe that spans exon 5 and 6 of full length *Tcf7l2* and detects all mRNA variants (assay ID: Mm00501505_m1). There was a significant effect of adipogenesis on total *Tcf7l2* mRNA overall (Fig. 1*D*), but it remained relatively stable during adipogenesis and was not correlated with the 58 or 78 kDa proteins ($P = 0.19$ and $P = 0.27$, respectively). Consistent with our 3T3-L1 data, TCF7L2 protein levels increased during differentiation of murine ASCs ex vivo, but there were no differences in the expression of the 58 or 78 kDa proteins in these cells (Fig. 1*E*).

TCF7L2 Expression Is Required for Adipogenesis

We generated stable 3T3-L1 preadipocytes with reduced TCF7L2 protein using lentivirus shRNA and examined the adipogenesis capacity of these cells. Silencing TCF7L2 protein led to an almost complete block of adipogenesis (Fig. 1*F*). Additional stable clones generated using different viral backbones and shRNA sequences that targeted alternate regions of *Tcf7l2* mRNA confirmed these findings (Supplementary Fig. 1). We did not observe effects of TCF7L2 silencing on cell proliferation, as determined by protein content and cell number on the day of adipogenesis induction (Supplementary Fig. 1). Consistent with impaired adipogenesis in shTCF7L2 cells, mRNA and protein induction of several adipogenic transcription factors (i.e., PPAR-γ and C/EBPα) were reduced in TCF7L2 silenced cells (Supplementary Fig. 2). Insulin- stimulated glucose uptake also was reduced in the shTCF7L2 adipocytes and was associated with intact insulin signaling at the level of $pAKT^{473}$ but with reduced Glut4 (*Slc2a4*) mRNA expression (Supplementary Fig. 3).

TCF7L2 Transcriptome in Adipocytes

We performed RNA-Seq analysis on stable shTCF7L2 3T3-L1 cells (clone shTCF7L2_A) at multiple time points during adipogenesis. In shTCF7L2 preadipocytes, we observed an upregulation of multiple inflammatory pathways that persisted for the duration of the adipogenesis time course (Fig. 2). These pathways were related to type I (interferon [IFN]-α) and type II (IFN-γ) IFN responses and complement pathway activity (Fig. 2 and Supplementary Data). Inflammatory gene upregulation was not related to specific shRNA or plasmid sequences because a selection of differentially expressed genes was confirmed using quantitative real-time PCR in independent shTCF7L2 clones using alternate shRNA sequences and plasmids (Supplementary Fig. 4). In contrast, the expression of genes involved in important metabolic processes, including fatty acid, bile acid, and cholesterol metabolism, were reduced. Pathways involved in epithelial-to-mesenchymal transition (EMT) and angiogenesis were downregulated in preadipocytes, consistent with important developmental roles for Wnt signaling in these pathways (Fig. 2 and Supplementary Data).

Wnt Signaling During Adipogenesis

GSEA analysis indicated that the Wnt/β-catenin signaling pathway was not significantly altered in shTCF7L2 3T3L1 cells. However, a number of Wnt genes and targets were differentially expressed in our RNA-Seq data set (Supplementary Data), and highly related GSEA pathways were altered in shTCF7L2 cells, including Myc target, Notch, and Hedgehog pathways (Fig. 2). Thus, to characterize Wnt signaling in more detail, we examined the mRNA expression of a number of key Wnt genes. The expression of *Axin2*, a transcriptional marker of Wnt pathway activation (25,26), was relatively low in control cells, fluctuated moderately during adipogenesis, but was increased approximately sevenfold in shTCF7L2 cells (Fig. 3*A*). Interestingly, the expression of lymphoid enhancer-binding factor 1 (*Lef1*), a key member of the high-mobility group (HMG)-box family of Wnt transcription factors, increased sharply during

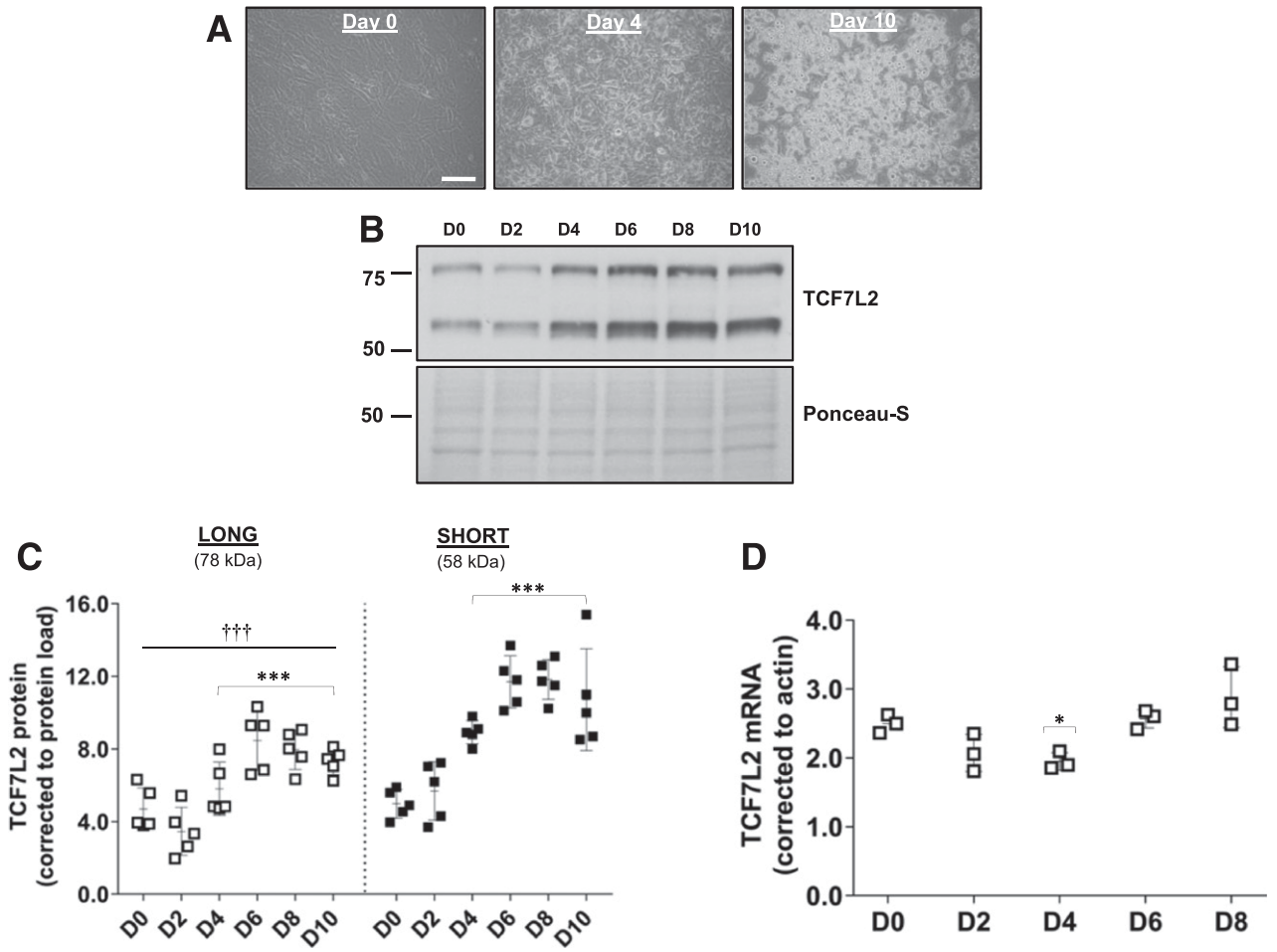

Figure 1—*A*: Representative images of differentiating 3T3-L1 adipocytes at the time of induction, day 0 (D0), and at D4 and D10 after initiation of adipogenesis (scale bar = 100 μm). *B* and *C*: A representative Western blot of TCF7L2 during adipogenesis, examined using an antibody that recognizes an epitope around Leu331 and all variants of TCF7L2. The expression of the short (58 kDa) TCF7L2 protein isoform was higher than the long (78 kDa) isoform during adipogenesis. Total protein load, assessed by Ponceau-S staining, was used for normalization (n = 5 independent experiments). ***$P < 0.001$ vs. D0 by two-way ANOVA Holm-Šidák multiple comparison t test; †††$P < 0.001$ main difference between isoform expression by two-way ANOVA. *D*: Total *Tcf7l2* mRNA quantified by quantitative real-time PCR using a TaqMan probe (assay ID: Mm00501505_m1) reached a nadir at D4 after induction of adipogenesis before recovering to baseline levels at day 8 (n = 3 independent experiments). $P < 0.01$ effect of time by one-way ANOVA: *$P < 0.05$ vs. D0 by Holm-Šidák multiple comparison t test. *E*: Representative images of differentiating murine ASCs at D0, D2, and D6 after initiation of adipogenesis (scale bar = 100 μm). Representative Western blot of TCF7L2 demonstrates increased TCF7L2 protein during adipogenesis. The expression of the 58 kDa TCF7L2 protein was similar to the 78 kDa protein during adipogenesis (n = 5 independent experiments). ***$P < 0.001$ vs. D0 by two-way ANOVA Holm-Šidák multiple comparison t test. *F*: TCF7L2 silencing in 3T3-L1 cells (shTCF7L2) inhibited adipogenesis. A Western blot of TCF7L2 from three replicate shTCF7L2 D0 cells is shown to demonstrate the efficiency of TCF7L2 silencing. The differentiation capacity of shTCF7L2 preadipocytes was assessed by triglyceride accumulation (n = 4 independent adipogenesis experiments). ***$P < 0.001$ t test vs. shSCR. Note these triglyceride data also are included in Supplementary Fig. 1 (shTCF7L2_A) for comparison with other stable shTCF7L2 clones. (A high-quality color representation of this figure is available in the online issue.)

adipogenesis in control cells, which was attenuated by TCF7L2 silencing (Fig. 3*A*). The levels of *Myc* peaked early on day 2, where *Myc* was increased ~10-fold compared with preadipocytes. Consistent with the GSEA data, the induction of Myc expression during adipogenesis was significantly blunted (Fig. 3*A*). The mRNA levels of WNT1-inducible-signaling pathway protein 2 (*Wisp2*), a novel secreted adipokine and Wnt pathway activator (27), were elevated during adipogenesis in shTCF7L2 cells (Fig. 3*A*). Consistent with previous reports (28), transducin-like enhancer of split 3 (*Tle3*) mRNA increased during adipogenesis in control cells, but its expression was significantly attenuated in shTCF7L2 cells (Fig. 3*A*). The mRNA levels of β-catenin (*Ctnnb1*) were moderately affected by adipogenesis but were not significantly different in shTCF7L2 cells (Fig. 3*A*). In contrast to these mRNA data, total and active β-catenin protein were highly expressed in preadipocytes and declined during adipogenesis (Fig. 3*B*). Total β-catenin protein levels were lower in shTCF7L2 cells, but active β-catenin levels were unchanged, resulting in an increase in the active-to-total β-catenin ratio in shTCF7L2 cells (Fig. 3*B*).

To explore the role of β-catenin in the inhibition of adipogenesis in shTCF7L2 cells, we treated cells with

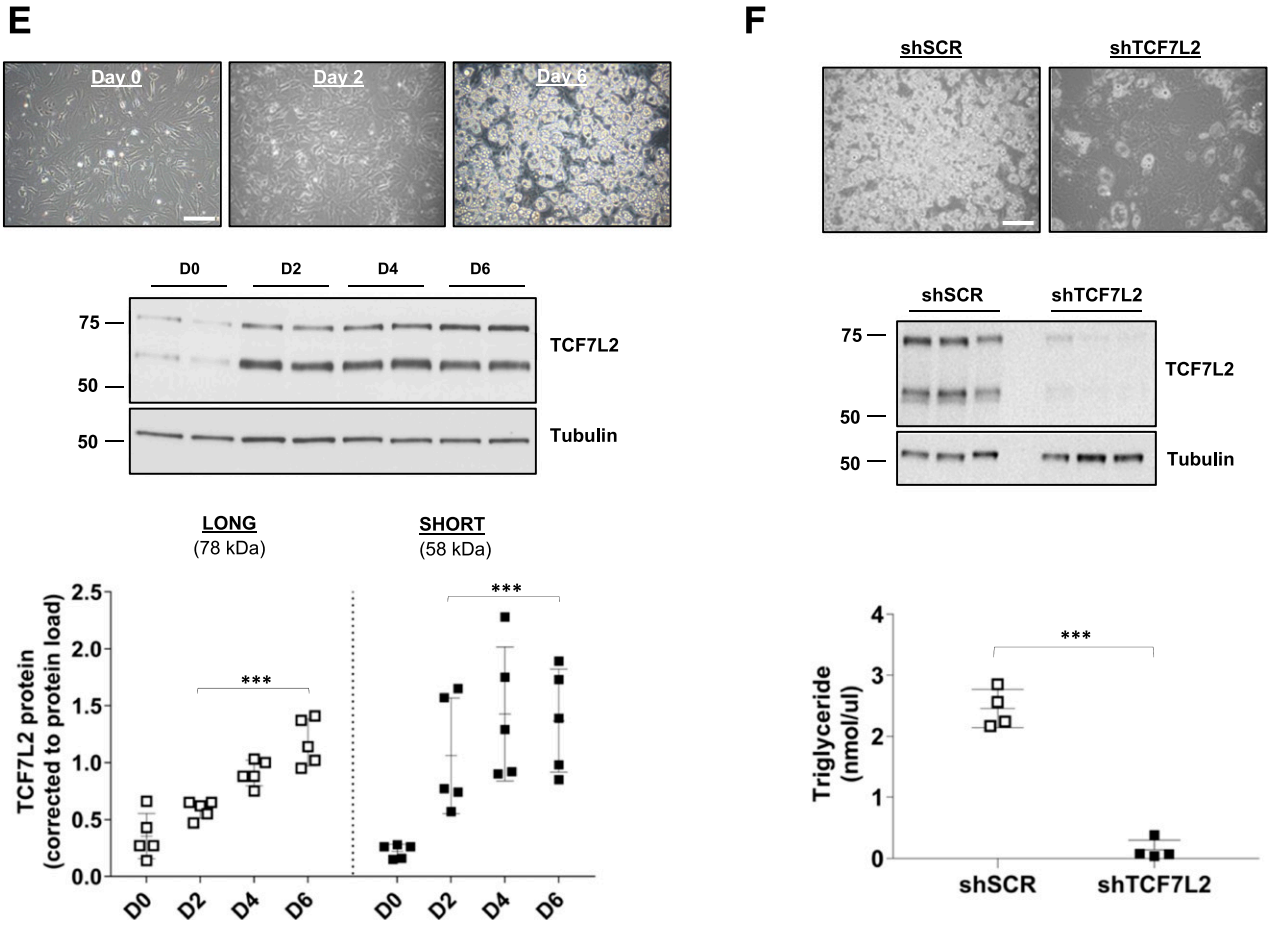

Figure 1—*Continued*.

IWR-1, a small molecule endogenous Wnt signaling antagonist that stabilizes the β-catenin destruction complex (29). In high passage (passage 8) preadipocyte 3T3-L1 cells with submaximal adipogenesis, IWR-1 treatment led to β-catenin degradation, increased *Pparg* mRNA and a twofold increase in adipogenesis (Fig. 3*C*). This was associated with elevated *Lef1* expression, consistent with our data showing increased *Lef1* mRNA during adipogenesis. However, IWR-1 was unable to restore adipogenesis in shTCF7L2 cells despite similarly robust β-catenin degradation (Fig. 3*C*). Moreover, the effect of IWR-1 on *Lef1* and *Pparg* expression was blocked, and the marked increase in *Axin2* mRNA persisted in shTCF7L2 cells (Fig. 3*C*). Taken together, these data suggest that the regulation of Wnt signaling during adipogenesis is disturbed in the absence of TCF7L2 expression and indicate that TCF7L2 expression is required for adipogenesis.

Generation of Adipocyte-Specific ΔE11-TCF7L2 Mice

We next investigated the role of TCF7L2 in mature adipocytes in vivo. Adipoq-Cre mediated excision of exon 11 of *Tcf7l2*, which is common to all *Tcf7l2* mRNA variants and encodes the DNA binding domain of TCF7L2, led to the expression of *Tcf7l2* mRNA lacking exon 11 only (Fig. 4*A* and *B*). This functionally inactivates TCF7L2 and blocks TCF7L2-mediated Wnt signaling, and whole-body ΔE11-TCF7L2 mice display an identical phenotype to the classic *Tcf7l2*-knockout mice (19,30). Three-month-old male and female ΔE11-TCF7L2 mice were not significantly heavier than control littermates, and there was no difference in total or lean fat mass, as assessed in females (Supplementary Fig. 5). However, female mice had increased food intake and lower fasting leptin. The increased food intake in female mice was offset by an increase in activity because the net energy balance was not significantly increased in these mice (Supplementary Fig. 5).

Glucose Homeostasis in ΔE11-TCF7L2 Mice

At 3 months of age, male (Fig. 4*D* and *E*) and female (Supplementary Fig. 6) chow-fed ΔE11-TCF7L2 mice were glucose intolerant compared with age-matched LoxP/LoxP control mice. The ΔE11-TCF7L2 mice displayed early hyperinsulinemia during the IPGTT (Fig. 4*F*) and were insulin resistant, as determined by ITTs (Supplementary Fig. 6). No difference was observed in glucose tolerance between LoxP/LoxP control mice and Adipoq-Cre mice (data not shown), consistent with previously published findings (31). Because male and female mice displayed

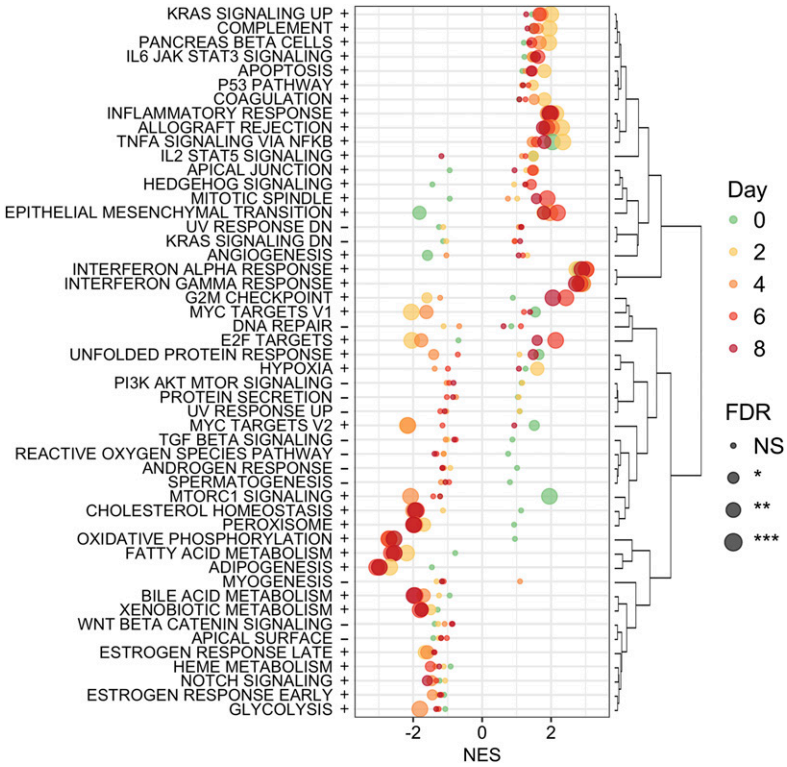

Figure 2—Hallmark GSEA from RNA-Seq experiments performed on shSCR and shTCF7L2 3T3-L1 cells in preadipocytes at day 0 and at days 2, 4, 6, and 8 during adipogenesis. Normalized enrichment scores (NES) from GSEA across all time points. The 50 hallmark gene sets were hierarchically clustered in R software using heatmap.2 from gplots and Euclidean distance to obtain the gene set ordering and the dendrogram used in the plot. The dot color indicates the time point and dot size the statistical significance (GSEA FDR), as indicated in the figure legend. *$P <$ 0.05; **$P < 0.01$; ***$P < 0.001$, and NS. Between the gene sets names and the plot, + and − indicate whether the gene set had an FDR <0.05 at any time point (+) or not (−).

similar glucose tolerance phenotypes, further studies were performed in males.

We used low-dose hyperinsulinemic-euglycemic clamps with a [3-^{3}H]glucose infusion to accurately quantitate basal and insulin-stimulated glucose R_a and R_d. Consistent with our IPGTT data, the glucose infusion rate was reduced during the clamp in ΔE11-TCF7L2 mice (Fig. 4*G*). Basal glucose R_a and R_d were not different in ΔE11-TCF7L2 mice (Fig. 4*H*), but we did observe increased insulin-stimulated R_a (Fig. 4*I*), confirming hepatic insulin resistance in 3-month-old TCF7L2-mutant mice. This phenotype was not associated with hepatic steatosis in the chow-fed male mice but was associated with increased expression of fasting hepatic stearoyl-CoA desaturase-1 (*Scd1*) and elevated mRNA levels of several gluconeogenic genes (*G6pc*, *Pck1*, and *Pcx*) at the end of the insulin clamp (Supplementary Figs. 5 and 7).

To examine the mechanisms underlying hepatic insulin resistance in ΔE11-TCF7L2 mice, we fed mice the 60% HFD for 12 weeks. Cumulative weight gain during the HFD in ΔE11-TCF7L2 mice was not significantly different (Fig. 5*A*), but ΔE11-TCF7L2 mice were significantly heavier in absolute body weight at the end of the diet, despite similar cumulative food intake (Fig. 5*B–D*). Glucose intolerance in ΔE11-TCF7L2 mice progressed after the HFD to include fasting and 2 h hyperglycemia (Fig. 5*E* and *F*). HFD-fed ΔE11-TCF7L2 mice also displayed hepatomegaly (not shown), increased lipid deposition on hematoxylin and eosin sections, and increased hepatic triglycerides (Fig. 5*G* and *H*). These data demonstrate that TCF7L2 inactivation in mature adipocytes promotes hepatic insulin resistance in chow- and HFD-fed mice. In HFD-fed animals, this may at least partially be explained by an increase in lipid deposition in liver.

Adipose Tissue Morphology in ΔE11-TCF7L2 Mice

At 3 months of age there was a small increase in inguinal white adipose tissue (iWAT) mass in male ΔE11-TCF7L2 mice, but this was not statistically significant (Fig. 6*A*). By 6 months of age, iWAT weight was 2.5-fold larger in ΔE11-TCF7L2 mice, which was maintained after the HFD (Fig. 6*A*). A significant shift toward larger adipocytes was already detectable in the younger mice. There was a reduction in smaller adipocytes (500–1,000 μm^2) and a significant increase in the proportion of adipocytes larger than 4,000 μm^2 (Fig. 6*B* and *D*). This was exacerbated in older mice where, on average, adipocytes were ~twofold larger compared with controls (Fig. 6*C* and *E*). The adipocyte area in these mice was highly correlated with iWAT weight (Fig. 6*G*), and we counted fewer adipocytes in the same total

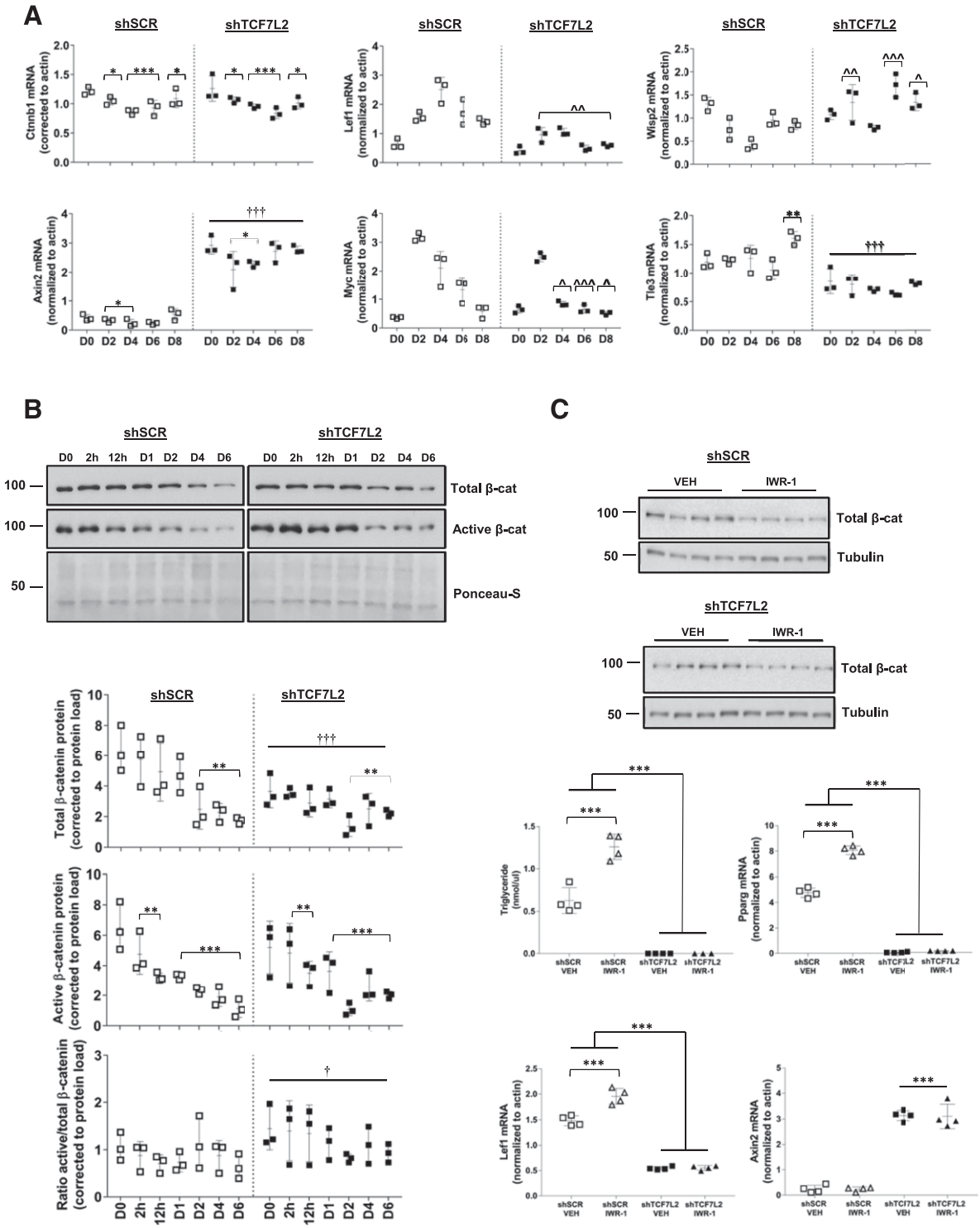

Figure 3—*A*: The mRNA expression of Wnt genes *Cttnb1, Axin2, Lef1, Myc, Wisp2*, and *Tle3* during adipogenesis in shTCF7L2 and shSCR control cells. *B*: Representative Western blot and corresponding quantification for total and active β-catenin protein during adipogenesis in shSCR and shTCF7L2 3T3-L1 cells ($n = 3$ independent experiments). *$P < 0.05$; **$P < 0.01$; ***$P < 0.001$ vs. day (D) 0 by two-way ANOVA Holm-Šidák multiple comparison *t* test; †$P < 0.05$ main effect of shTCF7L2 by two-way ANOVA. †††$P < 0.001$ main effect of shTCF7L2 by two-way ANOVA; ^$P < 0.05$; ^^$P < 0.01$; ^^^$P < 0.001$ vs. corresponding shSCR time point by two-way ANOVA time × shTCF7L2 interaction Holm-Šidák multiple comparison *t* test. *C*: Effect of IWR-1 treatment on total β-catenin levels and adipogenesis in high-passage shSCR and shTCF7L2 cells. Cells were treated with IWR-1 (10 μmol/L) every other day for 6 days during differentiation. Western blot demonstrates the effect of IWR-1 on total β-catenin protein levels at the end of adipogenesis (each lane represents a single independent adipogenesis experiment, $n = 4$ for each treatment). Triglycerides and the mRNA expression of *Pparg*, *Lef1*, and *Axin2* were assessed by quantitative real-time PCR at the end of differentiation on D6 ($n = 4$ independent differentiation experiments). ***$P < 0.001$ vs. indicated controls by two-way ANOVA interaction Holm-Šidák multiple comparison *t* test.

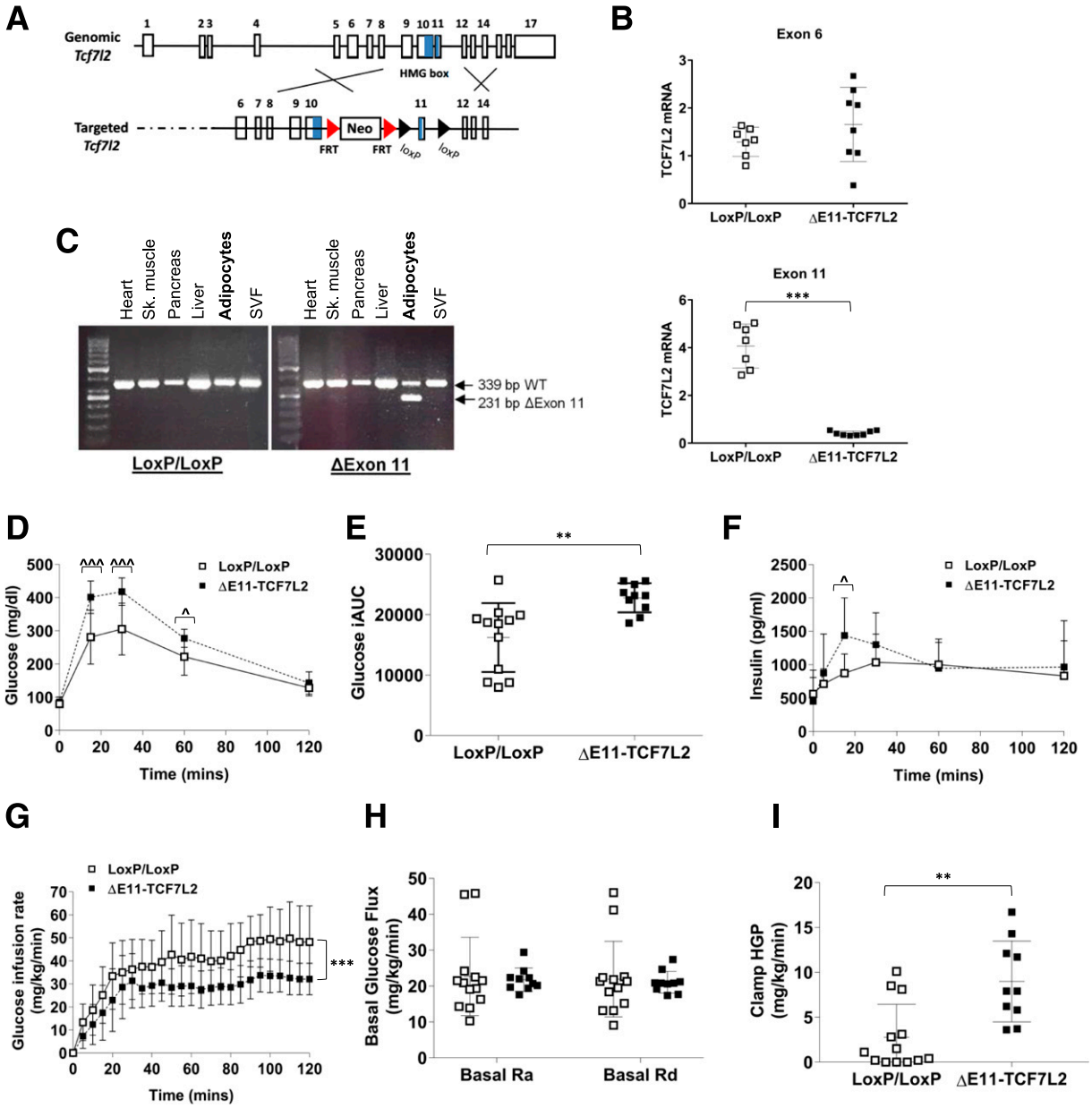

Figure 4—*A*: Schematic shows the targeting strategy for the mouse *Tcf7l2* locus used in this study. (Reprinted with permission from van Es et al. [19]) *B*: LoxP sites were placed around exon 11, which results in the deletion of exon 11, and not exon 6, containing mRNA transcripts, as determined by quantitative real-time PCR on isolated adipocytes (n = 7). ***$P < 0.001$ vs. LoxP control mice by Welch t test. The exon 11–specific quantitative real-time PCR probe/primer combination was custom designed by Integrated DNA Technologies (Coralville, IA). *C*: To confirm deletion of exon 11 was specific to adipocytes, semiquantitative RT-PCR was used to visualize *Tcf7l2* transcripts in multiple tissues. Recombination of the *Tcf7l2* locus occurred only in adipocytes and not the stromal vascular fraction (SVF) of adipose tissue. *D*: IPGTT results (n = 10 ΔE11-TCF7L2, n = 12 LoxP controls). ^$P < 0.05$; ^^^$P < 0.001$ vs. corresponding control time point by two-way ANOVA time × *Tcf7l2* genotype interaction Holm-Šidák multiple comparison t test. *E*: Incremental area under the IPGTT curve (iAUC). **$P < 0.01$ by Welch t test. *F*: Plasma insulin during the IPGTT (n = 7 ΔE11-TCF7L2, n = 10 LoxP controls). ^$P < 0.05$ vs. corresponding control time point by two-way ANOVA time × genotype interaction Holm-Šidák multiple comparison t test. *G*: Glucose infusion rate. ***$P < 0.001$ main effect of *Tcf7l2* genotype by two-way ANOVA. Basal rate of glucose R_a and R_d (*H*) and residual insulin-stimulated hepatic glucose production (HGP) (*I*) during low dose hyperinsulinemic-euglycemic insulin clamps in male 3-month-old chow-fed mice (n = 10 ΔE11-TCF7L2, n = 13 LoxP control mice for all clamp experiments). **$P < 0.01$ vs. LoxP control mice by Mann-Whitney test.

histological area in the older ΔE11-TCF7L2 mice (Fig. 6*F*). Although 6-month-old mice were heavier and had increased whole-body fat mass, they had lower food intake, activity levels, and net energy expenditure (Supplementary Fig. 8). Thus, net energy balance was not significantly different in these mice. Interestingly, we also did not detect changes in the weight of the perigonadal visceral depot (pgWAT) examined after the HFD (Fig. 6*A*).

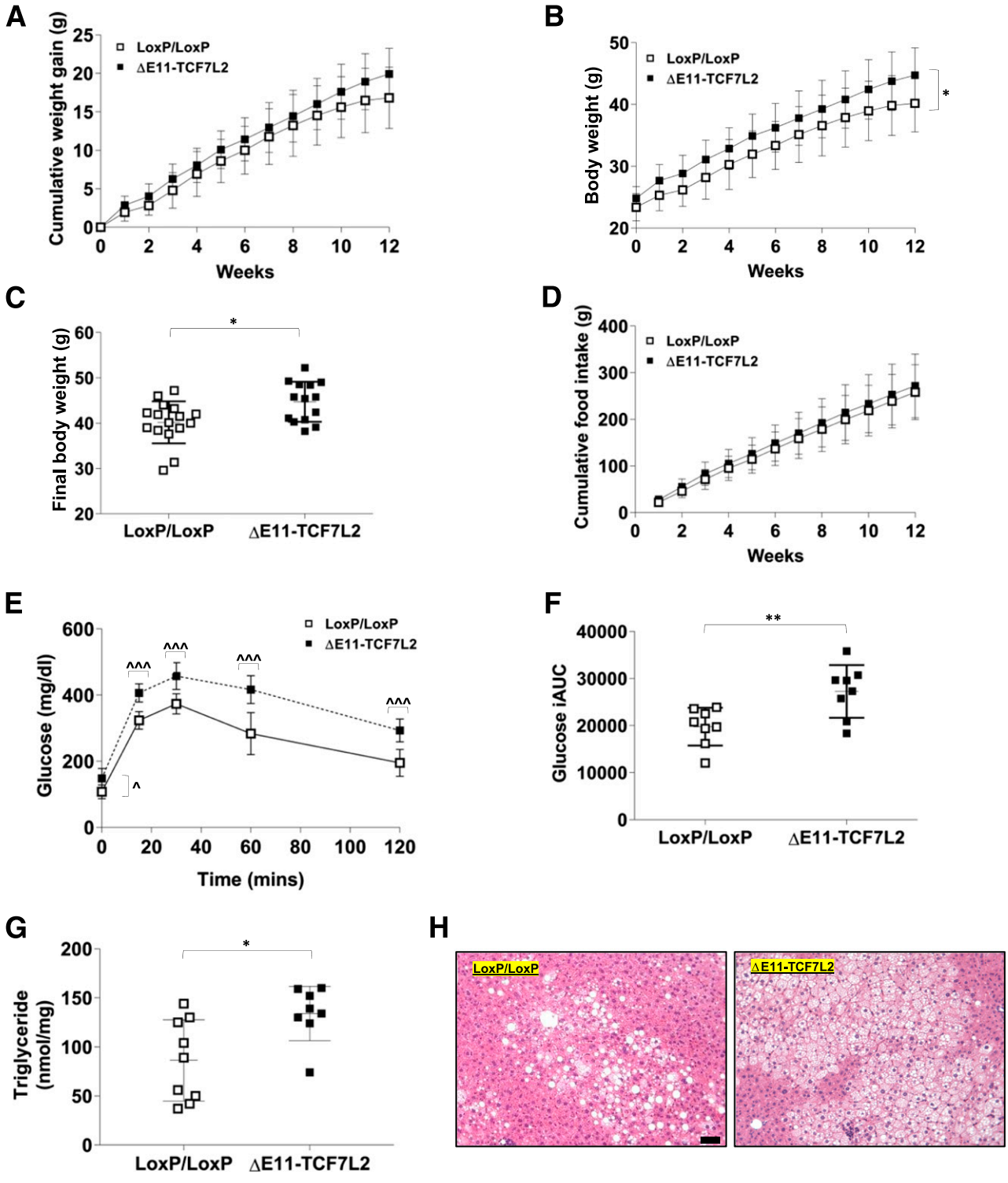

Figure 5—Cumulative weight gain (*A*), absolute body weight (*B*), final body weight (*C*), and cumulative food intake (*D*) during and after 12 weeks of the HFD ($n = 14$ ΔE11-TCF7L2, $n = 16$ LoxP controls). *$P < 0.05$ main effect of *Tcf7l2* genotype by two-way ANOVA (*B*); *$P < 0.05$ vs. controls by *t* test (*C*). IPGTT (*E*) and incremental area under the IPGTT curve (iAUC) after 12 weeks of the HFD in male mice ($n = 8$ ΔE11-TCF7L2, $n = 8$ control mice) (*F*). ^$P < 0.05$; ^^^$P < 0.001$ vs. corresponding control time point by two-way ANOVA time × *Tcf7l2* genotype interaction Holm-Šidák multiple comparison *t* test. **$P < 0.05$ vs. controls by *t* test. *G*: Liver triglyceride content was significantly elevated in ΔE11-TCF7L2 mice ($n = 8$ ΔE11-TCF7L2, $n = 9$ control mice). *$P < 0.05$ vs. controls by Mann-Whitney test. *H*: A representative hematoxylin and eosin stain demonstrates increased lipid deposition in liver in TCF7L2 mutant mice at the end of 12-week HFD (scale bar = 100 μm).

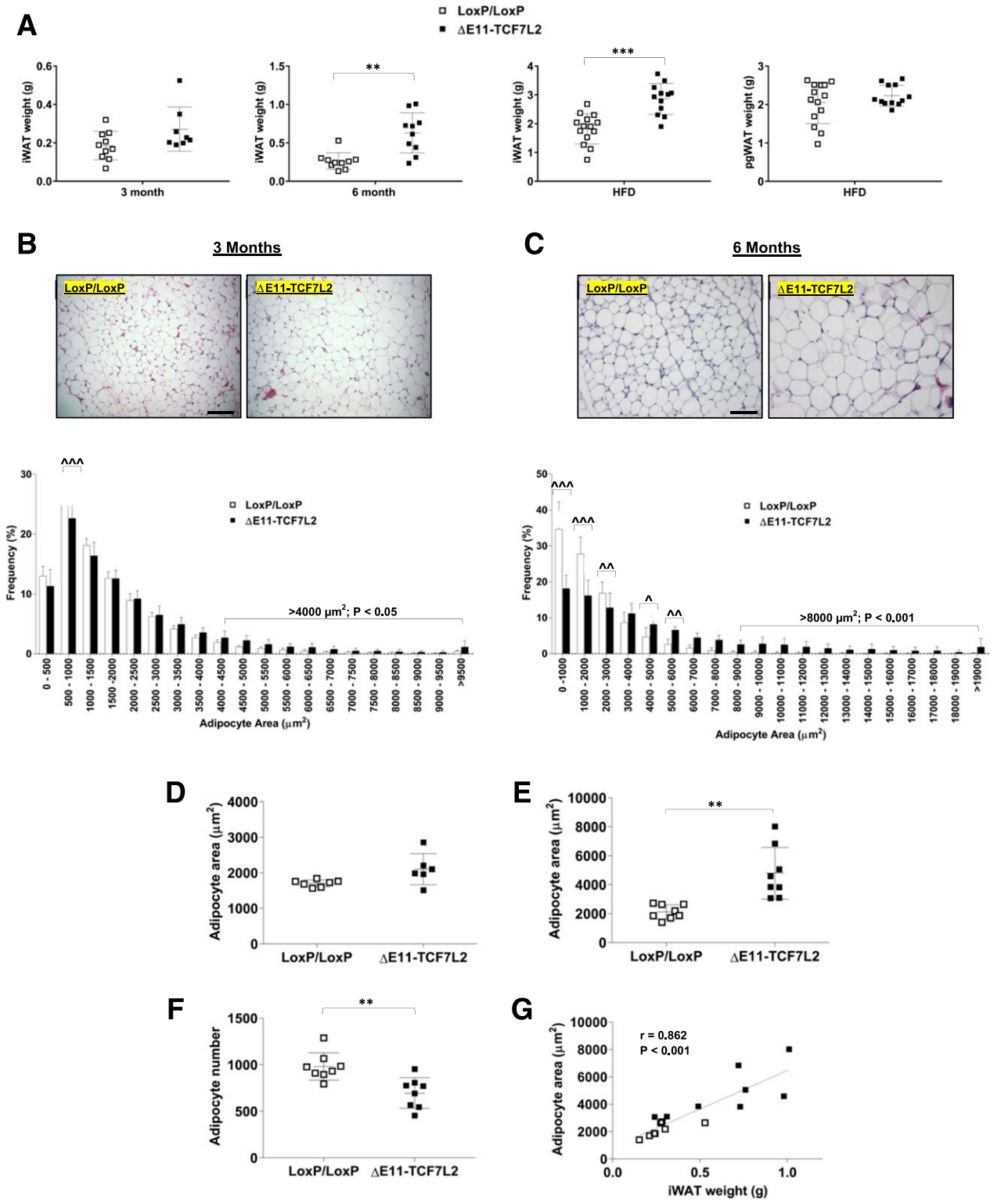

Figure 6—*A*: iWAT in male ΔE11-TCF7L2 mice at 3 and 6 months of age (n = 8–10 ΔE11-TCF7L2, n = 8–10 control mice) and iWAT and pgWAT after HFD (n = 12 ΔE11-TCF7L2, n = 14 control mice). $^{**}P < 0.01$ vs. control mice by Mann-Whitney test; $^{***}P < 0.001$ vs. control by t test. Representative hematoxylin and eosin stain and adipocyte size distribution performed on 3-month (*B*) and 6-month (*C*) iWAT (scale bar = 100 μm). Average adipocyte area in 3-month-old (n = 6 ΔE11-TCF7L2, n = 7 control mice) (*D*) and 6-month-old mice (n = 8 ΔE11-TCF7L2, n = 8 control mice) (*E*) was calculated using Adiposoft. $^{**}P < 0.01$ vs. control by Welch t test. *F*: Total number of adipocytes counted in an equal number of histological sections in 6-month-old mice. $^{**}P < 0.01$ vs. control by t test. *G*: Correlation between iWAT weight and adipocyte area in 6-month-old mice.

Adipocyte Gene Expression in ΔE11-TCF7L2 Mice

Consistent with our in vitro data, *Axin2*, complement factor H (*Cfh*) and MCP-1 (*Ccl2*) mRNA were increased in isolated adipocytes from HFD-fed mice, indicating adipocyte hypertrophy is associated with adipose tissue inflammation in ΔE11-TCF7L2 mice (Supplementary Fig. 9). Although *Pparg* mRNA was unchanged, we noted a marked increase in the expression of *Dgat2* mRNA, suggesting increased triglyceride synthesis/storage capacity in the hypertrophic adipocytes of ΔE11-TCF7L2 mice (Supplementary Fig. 9).

TCF7L2 Expression in Human Adipose Tissue

Finally, to examine the clinical significance of these findings we quantitated *TCF7L2* mRNA expression in adipose tissue biopsy samples from patients with NGT and IGT. The IGT subjects were matched for BMI but had significantly increased Adipo-IR (Fig. 7*D*). Total *TCF7L2* mRNA, detected using a TaqMan probe designed around exons 10 and 11 (assay ID: Hs01009038_m1) was significantly decreased in IGT subjects (Fig. 7*E*) as was the expression of a "full adipose tissue variant" (14) of *TCF7L2* that incorporates exons 12 and 13 (Fig. 7*F*).

DISCUSSION

In this study we demonstrate that the diabetes candidate gene and key Wnt pathway effector *Tcf7l2* has important developmental and metabolic roles in adipose tissue. Previous studies have demonstrated that overexpression of TCF7L2 lacking its β-catenin binding domain promotes spontaneous adipogenesis in preadipocyte 3T3-L1 cells and skeletal muscle precursor cells (4,5). These findings led to the conclusion that TCF7L2 impairs adipogenesis. However, we suspected this was a simplistic model of TCF7L2 and Wnt signaling activity during adipogenesis. First, several Wnt components, including TCF7L2 and multiple Wnt ligands and receptors, are expressed in mature, fully differentiated adipocytes (32,33). Second, the transcriptional activity of TCF7L2 is flexible based on its interaction with β-catenin and other transcriptional partners. In the absence of β-catenin binding, TCFs largely repress Wnt target genes via the recruitment of nuclear cofactors (34). Third, several secreted Wnt ligands, including Wnt4, Wnt5a, and Wnt5b, can stimulate adipogenesis (35,36). Lastly, our own preliminary data highlighted that TCF7L2 protein increased during adipogenesis in 3T3-L1 and primary ASCs.

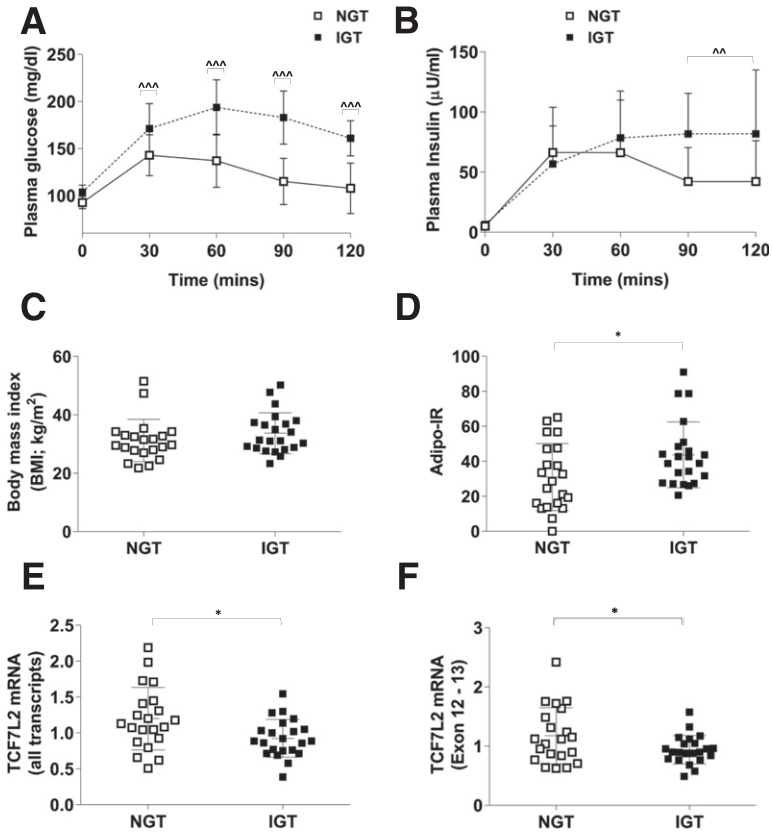

Figure 7—Plasma glucose (*A*) and insulin (*B*) during an oral GTT in human subjects with NGT ($n = 21$) or IGT ($n = 22$). ^^$P < 0.05$; ^^^$P < 0.001$ vs. corresponding NGT time point by two-way ANOVA time × NGT/IGT phenotype interaction Holm-Šidák multiple comparison *t* test. *C*: BMI was similar between the two groups. *D*: Adipo-IR was higher in IGT subjects. *$P < 0.05$ vs. NGT by *t* test. Subcutaneous adipose tissue total *TCF7L2* mRNA (exon 10-11; assay ID: Hs01009038_m1) (*E*) and a short *TCF7L2* mRNA variant incorporating exons 12 and 13 (*F*) were lower in IGT subjects with Adipo-IR. *$P < 0.05$ Welch *t* test vs. NGT.

Our cellular studies showed that stable silencing of TCF7L2 impaired adipogenesis. This was associated with disruption of Wnt signaling, as indicated by a significant upregulation of *Axin2* mRNA and changes in the expression of multiple Wnt genes, including *Lef1*, *Myc*, and *Wisp2*. However, the effects of TCF7L2 silencing on β-catenin levels were relatively modest in comparison. Although we did observe a significant increase in the ratio of active-to-total β-catenin, the levels of both proteins fell significantly during adipogenesis in control and shTCF7L2 cells. Furthermore, in rescue experiments using the Wnt inhibitor IWR-1, Wnt pathway inhibition through β-catenin degradation enhanced adipogenesis in control cells, but this effect was blocked in shTCF7L2 cells. These data, and the persistent alterations in the expression of *Axin2* and *Lef1* in IWR-1–treated shTCF7L2 cells, raise the interesting possibility that TCF7L2 may have β-catenin–dependent and –independent roles in adipocytes, which may vary temporally during adipogenesis. For example, in developing and mature adipocytes, where β-catenin levels are relatively low, increasing TCF7L2 expression may suppress Wnt pathway activation and promote adipogenesis. In contrast, in preadipocytes, low TCF7L2 levels and high β-catenin may permit Wnt activation and inhibit adipocyte development. This bidirectional feature of TCFs has been demonstrated in classic Wnt signaling studies performed in *Drosophila*, *Xenopus*, and *Caenorhabditis elegans* (34). In support of this putative temporal relationship between β-catenin and TCF7L2 during adipogenesis, a previous study demonstrated that co-occupancy of TCF7L2 and β-catenin decreases at the *Fabp4* promotor as adipogenesis progresses (28). Furthermore, *Tle3* suppresses Wnt signaling, displaces β-catenin bound to TCF7L2, and promotes adipogenesis (28). Our data demonstrate that *Tle3* mRNA levels are significantly reduced in shTCF7L2 cells, which further suggests an important interaction between these two proteins to facilitate adipogenesis.

Taken together, these findings may be difficult to reconcile with those from studies overexpressing dominant negative TCF7L2 in preadipocytes, where increased adipogenesis was observed (4). A potential explanation for this discrepancy is that overexpression of TCF7L2 that lacks β-catenin binding functionality does not block all transcriptional activity of TCF7L2. On the contrary, high levels of β-catenin–binding mutants of TCF7L2 are still able to bind gene promotors and, as discussed above, can interact with alternate transcriptional partners to promote the expression of proadipogenic genes. Thus, our data do not dispute the well-established finding that Wnt signaling per se impairs adipogenesis but instead highlight a far more complex regulatory role for TCF7L2 during adipogenesis that may depend on the balance between TCF7L2 and β-catenin levels, the timing of their interaction, and the interaction between TCF7L2 and other cofactors at specific gene promoters. Further highlighting this complexity, in 3T3-L1 cells, the shorter TCF7L2 protein was dominant in developing and mature adipocytes, consistent with a recent report (10). This isoform differs only in its C-terminus and retains all functional domains of full-length TCF7L2 (37). Clearly, the regulation of adipose tissue development by TCF7L2 and the role that β-catenin and Wnt signaling play in this process requires further study.

Despite clear differences in the expression of select Wnt genes, GSEA analysis of RNA-Seq data did not identify the Wnt pathway as differentially regulated in shTCF7L2 cells. There are several explanations for this. First, significant overlap exists between the Wnt pathway gene set and related pathways that were altered in shTCF7L2 cells and that contain a number of Wnt genes. This was most apparent for the Myc target (which includes *Myc*), Notch (which includes *Tcf7l2*, *Fzd1*, *Fzd5*, *Wnt2*, and *Wnt5a*), and Hedgehog (which includes *Tle3*) GSEA pathways. Second, many Wnt genes and targets, including *Tcf7l2* and *Ctnnb1*, are regulated posttranslationally during adipogenesis. Third, the GSEA pathway gene set for Wnt signaling does not include a number of key Wnt-related genes that were altered during adipogenesis in shTCF7L2 cells, including *Tcf7l2*, *Wisp1*, *Wisp2*, and *Tle3*.

Interestingly, however, GSEA analysis did identify increased expression of inflammatory genes in shTCF7L2 preadipocytes. This may be an additional mechanism by which TCF7L2 impaired adipogenesis, because IFN signaling is a negative regulator of adipogenesis (38). We also noted increased expression of complement factor H in shTCF7L2 preadipocytes, which also has been shown to inhibit adipogenesis (39). The noncanonical branch of the Wnt signaling pathway has documented inflammatory roles in adipose tissue. In obese mice, Wnt5a ablation reduced adipose tissue inflammation and improved insulin resistance, whereas overexpression of Wnt5a in myeloid cells increased inflammation and impaired glucose tolerance (40). Consistent with these findings, secreted frizzled-related protein 5 (SFRP5), a Wnt5a antagonist, has been identified as an anti-inflammatory adipokine whose secretion is disrupted in obesity and T2DM (41). Despite replicating the effects of TCF7L2 silencing on inflammation using alternative plasmid and shRNA sequences, the possibility that these observations reflect off-target effects unrelated to TCF7L2 silencing cannot be dismissed completely in the current study.

Our in vivo data demonstrate that inactivation of TCF7L2 through deletion of its DNA binding domain in adipocytes specifically promotes whole-body glucose intolerance and hepatic insulin resistance. Under chow-fed conditions, the hepatic insulin resistance was not associated with overt hepatic lipotoxicity but was associated with increased expression of gluconeogenic genes after the insulin clamp and increased fasting *Scd1* levels. The increase in hepatic *Scd1* is noteworthy because it has important roles in the early onset of lipid-induced hepatic insulin resistance and directly regulates hepatic glucose production through the expression of *Pck1* and *G6pc* (42). The TCF7L2-mutant mice also displayed significant alterations in adipocyte size distribution in iWAT. This was already detectable in younger mice with glucose intolerance, but without significant

increases in iWAT mass, and further progressed in 6-month-old mice that had a twofold increase in iWAT mass. The precise mechanisms of adipocyte hypertrophy are unclear but may reflect a combination of reduced hyperplasia and increased lipid synthesis/storage, two processes that are reciprocally regulated in adipose tissue (43). Increased lipid synthesis/storage may be secondary to elevated *Dgat2* expression, which we observed in adipocytes from HFD-fed ΔE11-TCF7L2 mice. This enzyme is rate limiting for triglyceride synthesis in adipocytes, its expression is closely correlated with hypertrophic adipocyte expansion (44,45), and we previously showed that it is a direct transcriptional target of TCF7L2 (18). A direct effect of TCF7L2 inactivation in preadipocytes in vivo is unlikely to contribute to the unhealthy adipose tissue expansion observed in TCF7L2-mutant mice. Adiponectin is expressed in mature adipocytes only, and Adipo-Cre–mediated recombination of the *Tcf7l2* gene was not observed in the stromal vascular fraction. Thus, alternative mechanisms may indirectly regulate ASC recruitment and differentiation in ΔE11-TCF7L2 mice. We detected increased expression of *Ccl2* and *Cfh* gene expression in hypertrophic adipocytes from TCF7L2-mutant mice, and CCL2 (MCP-1) inhibits adipocyte growth and differentiation (46). Moreover, increased *Axin2* mRNA suggests increased adipocyte Wnt activity in hypertrophic adipocytes from ΔE11-TCF7L2 mice. This may be an additional mechanism regulating adipose tissue expansion in these mice because several Wnt ligands have potent effects on adipogenesis in vitro and in vivo (47–50).

Interestingly, we did not detect increased pgWAT mass in ΔE11-TCF7L2 mice. This is consistent with previous studies demonstrating that the Wnt pathway differentially regulates adipose tissue depot formation (51) and may reflect the distinct developmental origins of these fat compartments (52). We also did not observe significant changes in energy balance in TCF7L2-mutant mice. Long-term energy balance analysis over the course of weeks or months, not examined in the current study, might possibly have revealed differences in energy balance in TCF7L2-mutant mice. It is interesting that whole-body heterozygote *Tcf7l2*-knockout mice have reduced fat mass, suggestive of impaired adipogenesis, but improved glucose tolerance (53,54). However, the glucose tolerance in whole-body *Tcf7l2* mutants may not reflect the role of TCF7L2 in adipose tissue alone, but rather TCF7L2 action in other metabolic tissues (3). Numerous studies have demonstrated that TCF7L2 regulates hepatic glucose metabolism (55,56), β-cell mass, and insulin secretion (57).

In humans, the effect of the TCF7L2 risk allele on T2DM is modulated by obesity, and T2DM prevalence is higher in nonobese carriers (11,12). Moreover, *TCF7L2* SNPs have been associated with obesity (58), but this association remains controversial and may be the result of ascertainment bias (59). However, a recent study showed weight loss after gastric bypass surgery led to the differential expression of *TCF7L2* mRNA isoforms in subcutaneous fat (14). Total *TCF7L2* mRNA was unchanged, but an adipose tissue–specific variant incorporating exons 12 and 13 was increased after surgery. Interestingly, the same study showed expression of a short TCF7L2 variant lacking exons 12 and 13 decreased after weight loss, was more common in subcutaneous fat of patients with T2DM, and correlated positively with free fatty acid during insulin clamps (14). In the current study, we demonstrate that total *TCF7L2* expression is reduced by ∼20% in adipose tissue from subjects with IGT and Adipo-IR. However, we did not observe differential expression of *TCF7L2* transcripts incorporating exon 12 and 13 because this variant also was reduced in IGT adipose tissue. These data are consistent with a previous study demonstrating reduced adipose tissue *TCF7L2* mRNA in patients with T2DM (60) and in carriers of the *TCF7L2* risk allele (61) and suggest that adipose tissue insulin sensitivity does not regulate *TCF7L2* gene splicing.

In conclusion, we show that TCF7L2 has important developmental and metabolic roles in adipose tissue. Using a combination of in vitro and in vivo techniques in cells from rodents and humans, we show that the regulation of adipogenesis by TCF7L2 and Wnt signaling is more complex than previously recognized and that inactivation of adipocyte TCF7L2 in vivo promotes adipocyte hypertrophy and peripheral and hepatic insulin resistance. Demonstrating the translational nature of our findings, we also show that adipocyte insulin resistance in humans is associated with a reduction in *TCF7L2* expression. We hope that further study of TCF7L2 and Wnt signaling in adipose tissue will provide more insights into the function of this important T2DM candidate gene.

Acknowledgments. The authors thank David H. Wasserman, Owen McGuinness, and Louise Lantier, at Vanderbilt Mouse Metabolic Phenotyping Center, and Syann Lee, at the Metabolic Core Unit at University of Texas Southwestern Medical Center in Dallas, for help in phenotyping.

Funding. This work was supported by National Institute of Diabetes and Digestive and Kidney Diseases grant K01-DK-098314 to L.N. and was partly supported by grants DK-059637 to the Vanderbilt Mouse Metabolic Phenotyping Center and DK-88761 to the Metabolic Core Unit at University of Texas Southwestern Medical Center in Dallas.

Duality of Interest. No potential conflicts of interest relevant to this article were reported.

Author Contributions. X.C. performed experiments, analyzed data, and reviewed and edited the manuscript. I.A., C.S., M.F., N.K.A., and C.P.J. researched data and reviewed and edited the manuscript. S.H. performed computational analysis and reviewed and edited the manuscript. L.N. planned the studies, performed experiments, analyzed all raw data, and wrote the manuscript. L.N. is the guarantor of this work and, as such, had full access to all the data in the study and takes responsibility for the integrity of the data and the accuracy of the data analysis.

Prior Presentation. Parts of this study were presented as an oral presentation at the 76th Scientific Sessions of the American Diabetes Association, New Orleans, LA, 10–14 June 2016.

References

1. Voight BF, Scott LJ, Steinthorsdottir V, et al.; MAGIC investigators; GIANT Consortium. Twelve type 2 diabetes susceptibility loci identified through large-scale association analysis. Nat Genet 2010;42:579–589

2. Jin T. Current understanding on role of the Wnt signaling pathway effector TCF7L2 in glucose homeostasis. Endocr Rev 2016;37:254–277
3. Nobrega MA. TCF7L2 and glucose metabolism: time to look beyond the pancreas. Diabetes 2013;62:706–708
4. Ross SE, Hemati N, Longo KA, et al. Inhibition of adipogenesis by Wnt signaling. Science 2000;289:950–953
5. Bennett CN, Ross SE, Longo KA, et al. Regulation of Wnt signaling during adipogenesis. J Biol Chem 2002;277:30998–31004
6. Kennell JA, MacDougald OA. Wnt signaling inhibits adipogenesis through beta-catenin-dependent and -independent mechanisms. J Biol Chem 2005;280: 24004–24010
7. Cawthorn WP, Bree AJ, Yao Y, et al. Wnt6, Wnt10a and Wnt10b inhibit adipogenesis and stimulate osteoblastogenesis through a β-catenin-dependent mechanism. Bone 2012;50:477–489
8. Liu J, Wang H, Zuo Y, Farmer SR. Functional interaction between peroxisome proliferator-activated receptor gamma and beta-catenin. Mol Cell Biol 2006;26: 5827–5837
9. Krishnan V, Bryant HU, Macdougald OA. Regulation of bone mass by Wnt signaling. J Clin Invest 2006;116:1202–1209
10. Tian L, Song Z, Shao W, et al. Curcumin represses mouse 3T3-L1 cell adipogenic differentiation via inhibiting miR-17-5p and stimulating the Wnt signalling pathway effector Tcf7l2. Cell Death Dis 2017;8:e2559
11. Cauchi S, Nead KT, Choquet H, et al. The genetic susceptibility to type 2 diabetes may be modulated by obesity status: implications for association studies. BMC Med Genet 2008;9:45
12. Corella D, Coltell O, Sorlí JV, et al. Polymorphism of the transcription factor 7-like 2 gene (TCF7L2) interacts with obesity on type-2 diabetes in the PREDIMED study emphasizing the heterogeneity of genetic variants in type-2 diabetes risk prediction: time for obesity-specific genetic risk scores. Nutrients 2016;8: 793
13. Nilsson E, Jansson PA, Perfilyev A, et al. Altered DNA methylation and differential expression of genes influencing metabolism and inflammation in adipose tissue from subjects with type 2 diabetes. Diabetes 2014;63:2962–2976
14. Kaminska D, Kuulasmaa T, Venesmaa S, et al. Adipose tissue TCF7L2 splicing is regulated by weight loss and associates with glucose and fatty acid metabolism. Diabetes 2012;61:2807–2813
15. Zebisch K, Voigt V, Wabitsch M, Brandsch M. Protocol for effective differentiation of 3T3-L1 cells to adipocytes. Anal Biochem 2012;425:88–90
16. Aune UL, Ruiz L, Kajimura S. Isolation and differentiation of stromal vascular cells to beige/brite cells. J Vis Exp 2013;(73):50191
17. Lakshmanan J, Elmendorf JS, Ozcan S. Analysis of insulin-stimulated glucose uptake in differentiated 3T3-L1 adipocytes. Methods Mol Med 2003; 83:97–103
18. Norton L, Chen X, Fourcaudot M, Acharya NK, DeFronzo RA, Heikkinen S. The mechanisms of genome-wide target gene regulation by TCF7L2 in liver cells. Nucleic Acids Res 2014;42:13646–13661
19. van Es JH, Haegebarth A, Kujala P, et al. A critical role for the Wnt effector Tcf4 in adult intestinal homeostatic self-renewal. Mol Cell Biol 2012;32:1918–1927
20. Ayala JE, Samuel VT, Morton GJ, et al.; NIH Mouse Metabolic Phenotyping Center Consortium. Standard operating procedures for describing and performing metabolic tests of glucose homeostasis in mice. Dis Model Mech 2010; 3:525–534
21. Kaiyala KJ, Schwartz MW. Toward a more complete (and less controversial) understanding of energy expenditure and its role in obesity pathogenesis. Diabetes 2011;60:17–23
22. Galarraga M, Campión J, Muñoz-Barrutia A, et al. Adiposoft: automated software for the analysis of white adipose tissue cellularity in histological sections. J Lipid Res 2012;53:2791–2796
23. Winnier DA, Fourcaudot M, Norton L, et al. Transcriptomic identification of ADH1B as a novel candidate gene for obesity and insulin resistance in human adipose tissue in Mexican Americans from the Veterans Administration Genetic Epidemiology Study (VAGES). PLoS One 2015;10:e0119941
24. Gastaldelli A, Gaggini M, DeFronzo RA. Role of adipose tissue insulin resistance in the natural history of type 2 diabetes: results from the San Antonio Metabolism Study. Diabetes 2017;66:815–822
25. Jho EH, Zhang T, Domon C, Joo CK, Freund JN, Costantini F. Wnt/beta-catenin/Tcf signaling induces the transcription of Axin2, a negative regulator of the signaling pathway. Mol Cell Biol 2002;22:1172–1183
26. Leung JY, Kolligs FT, Wu R, et al. Activation of AXIN2 expression by beta-catenin-T cell factor. A feedback repressor pathway regulating Wnt signaling. J Biol Chem 2002;277:21657–21665
27. Hammarstedt A, Hedjazifar S, Jenndahl L, et al. WISP2 regulates preadipocyte commitment and PPARγ activation by BMP4. Proc Natl Acad Sci U S A 2013;110: 2563–2568
28. Villanueva CJ, Waki H, Godio C, et al. TLE3 is a dual-function transcriptional coregulator of adipogenesis. Cell Metab 2011;13:413–427
29. Chen B, Dodge ME, Tang W, et al. Small molecule-mediated disruption of Wnt-dependent signaling in tissue regeneration and cancer. Nat Chem Biol 2009;5:100–107
30. Korinek V, Barker N, Moerer P, et al. Depletion of epithelial stem-cell compartments in the small intestine of mice lacking Tcf-4. Nat Genet 1998;19:379–383
31. Eguchi J, Wang X, Yu S, et al. Transcriptional control of adipose lipid handling by IRF4. Cell Metab 2011;13:249–259
32. Schinner S, Ulgen F, Papewalis C, et al. Regulation of insulin secretion, glucokinase gene transcription and beta cell proliferation by adipocyte-derived Wnt signalling molecules. Diabetologia 2008;51:147–154
33. Schinner S. Wnt-signalling and the metabolic syndrome. Horm Metab Res 2009;41:159–163
34. Bienz M. TCF: transcriptional activator or repressor? Curr Opin Cell Biol 1998; 10:366–372
35. van Tienen FH, Laeremans H, van der Kallen CJ, Smeets HJ. Wnt5b stimulates adipogenesis by activating PPARgamma, and inhibiting the beta-catenin dependent Wnt signaling pathway together with Wnt5a. Biochem Biophys Res Commun 2009; 387:207–211
36. Nishizuka M, Koyanagi A, Osada S, Imagawa M. Wnt4 and Wnt5a promote adipocyte differentiation. FEBS Lett 2008;582:3201–3205
37. Vacik T, Stubbs JL, Lemke G. A novel mechanism for the transcriptional regulation of Wnt signaling in development. Genes Dev 2011;25:1783–1795
38. McGillicuddy FC, Chiquoine EH, Hinkle CC, et al. Interferon gamma attenuates insulin signaling, lipid storage, and differentiation in human adipocytes via activation of the JAK/STAT pathway. J Biol Chem 2009;284:31936–31944
39. Moreno-Navarrete JM, Martínez-Barricarte R, Catalán V, et al. Complement factor H is expressed in adipose tissue in association with insulin resistance. Diabetes 2010;59:200–209
40. Fuster JJ, Zuriaga MA, Ngo DT, et al. Noncanonical Wnt signaling promotes obesity-induced adipose tissue inflammation and metabolic dysfunction independent of adipose tissue expansion. Diabetes 2015;64:1235–1248
41. Ouchi N, Higuchi A, Ohashi K, et al. Sfrp5 is an anti-inflammatory adipokine that modulates metabolic dysfunction in obesity. Science 2010;329:454–457
42. Gutiérrez-Juárez R, Pocai A, Mulas C, et al. Critical role of stearoyl-CoA desaturase-1 (SCD1) in the onset of diet-induced hepatic insulin resistance. J Clin Invest 2006;116:1686–1695
43. Faust IM, Johnson PR, Stern JS, Hirsch J. Diet-induced adipocyte number increase in adult rats: a new model of obesity. Am J Physiol 1978;235:E279–E286
44. Harris CA, Haas JT, Streeper RS, et al. DGAT enzymes are required for triacylglycerol synthesis and lipid droplets in adipocytes. J Lipid Res 2011;52:657–667
45. Suzuki R, Tobe K, Aoyama M, et al. Expression of DGAT2 in white adipose tissue is regulated by central leptin action. J Biol Chem 2005;280:3331–3337
46. Gerhardt CC, Romero IA, Cancello R, Camoin L, Strosberg AD. Chemokines control fat accumulation and leptin secretion by cultured human adipocytes. Mol Cell Endocrinol 2001;175:81–92
47. Gustafson B, Smith U. Activation of canonical wingless-type MMTV integration site family (Wnt) signaling in mature adipocytes increases beta-catenin levels and leads to cell dedifferentiation and insulin resistance. J Biol Chem 2010;285:14031–14041

48. Gustafson B, Smith U. The WNT inhibitor Dickkopf 1 and bone morphogenetic protein 4 rescue adipogenesis in hypertrophic obesity in humans. Diabetes 2012;61:1217–1224
49. Grünberg JR, Hoffmann JM, Hedjazifar S, et al. Overexpressing the novel autocrine/endocrine adipokine WISP2 induces hyperplasia of the heart, white and brown adipose tissues and prevents insulin resistance. Sci Rep 2017;7:43515
50. Christodoulides C, Lagathu C, Sethi JK, Vidal-Puig A. Adipogenesis and WNT signalling. Trends Endocrinol Metab 2009;20:16–24
51. Zeve D, Seo J, Suh JM, et al. Wnt signaling activation in adipose progenitors promotes insulin-independent muscle glucose uptake. Cell Metab 2012;15:492–504
52. Chau YY, Bandiera R, Serrels A, et al. Visceral and subcutaneous fat have different origins and evidence supports a mesothelial source. Nat Cell Biol 2014;16:367–375
53. Savic D, Ye H, Aneas I, Park SY, Bell GI, Nobrega MA. Alterations in TCF7L2 expression define its role as a key regulator of glucose metabolism. Genome Res 2011;21:1417–1425
54. Yang H, Li Q, Lee JH, Shu Y. Reduction in Tcf7l2 expression decreases diabetic susceptibility in mice. Int J Biol Sci 2012;8:791–801
55. Oh KJ, Park J, Kim SS, Oh H, Choi CS, Koo SH. TCF7L2 modulates glucose homeostasis by regulating CREB- and FoxO1-dependent transcriptional pathway in the liver. PLoS Genet 2012;8:e1002986
56. Ip W, Shao W, Song Z, Chen Z, Wheeler MB, Jin T. Liver-specific expression of dominant-negative transcription factor 7-like 2 causes progressive impairment in glucose homeostasis. Diabetes 2015;64:1923–1932
57. Mitchell RK, Mondragon A, Chen L, et al. Selective disruption of Tcf7l2 in the pancreatic β cell impairs secretory function and lowers β cell mass. Hum Mol Genet 2015;24:1390–1399
58. Locke AE, Kahali B, Berndt SI, et al.; LifeLines Cohort Study; ADIPOGen Consortium; AGEN-BMI Working Group; CARDIOGRAMplusC4D Consortium; CKDGen Consortium; GLGC; ICBP; MAGIC Investigators; MuTHER Consortium; MIGen Consortium; PAGE Consortium; ReproGen Consortium; GENIE Consortium; International Endogene Consortium. Genetic studies of body mass index yield new insights for obesity biology. Nature 2015;518:197–206
59. Stolerman ES, Manning AK, McAteer JB, et al. TCF7L2 variants are associated with increased proinsulin/insulin ratios but not obesity traits in the Framingham Heart Study. Diabetologia 2009;52:614–620
60. Cauchi S, Choquet H, Gutiérrez-Aguilar R, et al. Effects of TCF7L2 polymorphisms on obesity in European populations. Obesity (Silver Spring) 2008;16:476–482
61. Mondal AK, Das SK, Baldini G, et al. Genotype and tissue-specific effects on alternative splicing of the transcription factor 7-like 2 gene in humans. J Clin Endocrinol Metab 2010;95:1450–1457